JOURNAL OF AEROSPACE SOCIETY MALAYSIA

ARTICLE

EXPERIMENTAL FLUTTER ANALYSIS WITH BENDING-TORSION COUPLING

Nurul Zubaidah Zaki [1], Haris Ahmad Israr Ahmad [1,*] and Muhammad Faruq Foong [1]

1. Aeronautics Laboratory, Faculty of Mechanical Engineering, Universiti Teknologi Malaysia, 81310 UTM Skudai, Johor, Malaysia.

*Correspondence: harisahmad@utm.my

Abstract: In short, bending-torsion coupling is a phenomenon that occurs when bending and torsional deformations of a structure are coupled. This can happen due to the geometry of the structure or due to the aerodynamic forces acting on the structure. Bending-torsion coupling can have significant impact on the flutter onset conditions of a structure. This study aims to presents the results of an experimental analysis of flutter for composite wing with bending-torsion coupling. The experiment is conducted in the low-speed wind tunnel (UTM-LST), where the carbon fiber composite wing with fiber orientation of $[30°]_4$ and $[45°]_4$ are placed on the test rig to mimic real flight condition. An accelerometer sensor is used in the experiment to measure the wing model's structure vibration in x-, y- and z-axis. The results of the experiment have shown that the composite wing with fiber orientation of $[30°]_4$ has higher flutter speed, which can be contributed to the existence of bending-torsion coupling due to its fiber laminate orientation.

Keywords: flutter; aeroelasticity; bending-torsion coupling; composite wing; fiber orientation

1. Introduction

Flutter is arguably the most important of all aeroelastic phenomena and it is also the most difficult to predict. In short, flutter can be described as an unstable self-excited vibration in which the structure extracts energy from the air stream and it can potentially lead to a catastrophic structural failure [1]-[3]. Nowadays, advanced composites are widely used in the aircraft and wing structures due to their material properties [4]. It has been estimated that about 30% of the aircraft structures are made of various types of advanced composites [5]. Due to its directional properties, the composite structures could be tailored accordingly to alter the structural deformation and avoid flutter [6]. In this case, the tailoring is done by changing the fiber orientations to exploit its advantages such as high strength to weight ratio, effective stiffness and high resistance to dynamic instability [7]. Furthermore, the influence of bending-torsion coupling should also be included in the analysis of composite wing, unlike that for metallic structures where such coupling does not exist due to their isotropic nature [8]. In a previously conducted analysis on the effects of bending-torsion coupling towards divergence, it has been found that stiffness coupling could be employed to delay the onset of stall flutter [9]. Additionally, according to another conducted study, the composite tailoring involving bending-torsion coupling seems to be effective for high aspect ratio and low aspect ratio wings [10]. Since flutter results from the interaction between inertial, elastic and aerodynamic forces, the aeroelastic equation of motion is applied in the flutter speed computation [11]. In order to have a better prediction of flutter speed, a suitable aerodynamic theory must be chosen. Some researchers have used v-g method, k method and p-k method in flutter analysis [9, 11].

The purpose of this study is to determine the effects of bending-torsion coupling stiffness towards the flutter speed. Classical laminate theory (CLT) is used in this study to conduct a parametric study on laminate orientation and stacking sequence by considering the bending-torsion coupling rigidities. The

flutter speed is computed using the aeroelastic equation of motion by applying aerodynamic derivatives model and structural natural frequencies obtained from the finite element analysis. The data is validated by conducting experiment tests on the fabricated wing model with chosen laminate configurations. The experiment is conducted in the UTM low-speed wind tunnel.

2. Methodology

In this study, all three composite flat wing models used for the analysis are straight rectangular flat plates with different fiber orientations. All these composite wing models are fabricated using the same material of carbon fiber, which is Tenax-J HTS40 E13 3K 200tex by Composites Technology Research Malaysia (CTRM). The materials and geometry for all composite wings are respectively listed and shown in Table 1 and Figure 1.

Table 1: Material properties of Tenax-J HTS40 E13 3K

Parameters	**Value**
Young Modulus 0°, E_1	130 GPa
Young Modulus 90°, E_2	130 GPa
In-plane shear modulus, G_{12}	4 GPa
Poisson's ratio, ν_{12}	0.06
Density, ϱ	1770 kgm^{-3}
Thickness of one ply	0.0003 m
Grammage	200 gm^{-2}

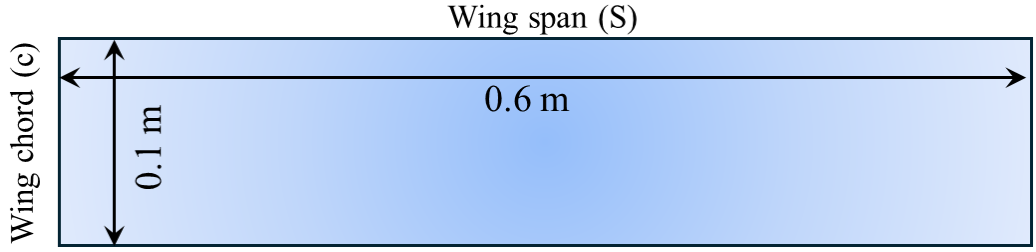

Figure 1: Composite flat wing geometry in this study

The selection of fiber orientation for the composite flat wing is conducted through a computational method with parameters obtained from [D] matrices derived from Classical laminate theory (CLT) as shown in Equation 1. From the theory, the bending-torsion coupling parameter can be obtained from the element D_{16}. Table 2 presents the bending stiffness matrix of each fiber orientation configuration varies from 0° to 45°. Moreover, calculation of bending-torsion coupling ratio is given by Equation 2.

$$\{M_x\ M_y\ M_{xy}\} = [D_{11}\ D_{12}\ D_{16}\ D_{12}\ D_{22}\ D_{26}\ D_{16}\ D_{26}\ D_{66}]\{k_x\ k_y\ k_{xy}\} \quad (1)$$

$$\text{Bending-torsion coupling ratio} = D_{16} \Big/ \sqrt{\frac{D_{11}}{D_{66}}} \quad (2)$$

Variation of the bending-torsion stiffness coupling ratio against the fiber orientation is illustrated in Figure 2. From Figure 2, it is found that the highest bending-ratio coupling is between 10° and 30°. In contrast, the fiber orientation of 0° and 45° resulted in 0 coupling ratio, which indicates that there is no coupling between bending and torsion stiffness. Hence, in this study, the chosen composite laminate

configurations are $[30°]_4$ and $[45°]_4$ that respectively represent the sample with the existence and non-existence of the bending-torsion coupling parameters.

Table 2: Parameters of [D] as defined from CLT

Fiber Orientation (θ°)	D_{11} (GPa.mm^3)	D_{12}	D_{16}	D_{22}	D_{26}	D_{66}
$[0_4]$	1.88	0.113	0.000	1.88	0.00	0.0576
$[5_4]$	1.85	0.138	0.141	1.85	-1.41	0.0825
$[10_4]$	1.78	0.209	0.265	1.78	-2.65	0.0154
$[15_4]$	1.67	0.319	0.357	1.67	-3.57	0.0264
$[20_4]$	1.54	0.454	0.406	1.54	-4.06	0.0399
$[25_4]$	1.39	0.597	0.406	1.39	-4.06	0.0542
$[30_4]$	1.26	0.732	0.357	1.26	-3.57	0.0677
$[35_4]$	1.15	0.842	0.265	1.15	-2.65	0.0787
$[40_4]$	1.08	0.913	0.141	1.08	-1.41	0.0858
$[45_4]$	1.05	0.938	0.000	1.05	0.00	0.0883

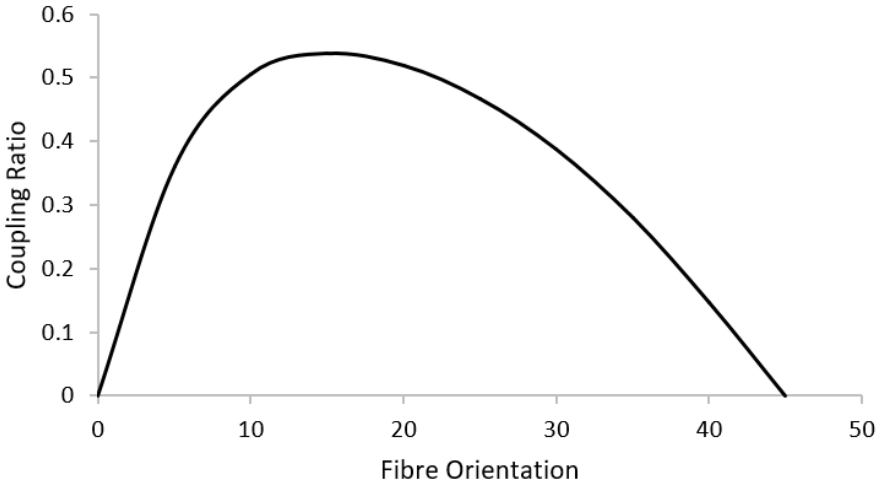

Figure 2: Bending-torsion coupling ratio at different fibre orientation

In the experimental tests, the composite flat wing models are installed on the test rig and placed in the wind tunnel test section. An accelerometer is used in this study to measure the acceleration of the wing root in three axes of direction: the x- and y- coordinate axes and direction of the air stream, which are indicated in Figure 3. During the experimental tests, wind tunnel velocity is systematically increased from an initial value of 0 m/s to the final value of 20 m/s. The occurrence of flutter speed is carefully monitored, which signifies the onset of oscillatory and vibratory behavior in the wing model's structure. Therefore, during the flutter point, the accelerometer data will show significant changes in the voltage in the three different axes. To ensure precision and minimize experimental errors, the composite wing model undergoes three consecutive test iterations. This approach aims to enhance accuracy and reduce potential reading errors during the experiment.

Figure 3: Experimental set-up in the test section of the wind tunnel

It should be noted that the experimental test rig is constructed to serve as a horizontal and rigid apparatus, acting as the support structure for the composite wing to replicate its behavior during flight. It is made as a rigid holder with various sections that may be adjusted to hold the wing at various angles of attack. This configuration facilitates the passage of air through the wing model, thus demonstrating the phenomenon of flutter that occurs when the wind velocity reaches the flutter limit.

3. Results and Discussion

Through the geometrical and material setup in the pre-processing of the ABAQUS software, the free vibration analysis of the composite flat wing structure with the laminate stacking sequences of $[\theta]_4$ different fiber orientations are conducted. From Table 3, the first four structural natural frequencies for each fiber orientation are presented. On the other hand, Figure 4 and Figure 5 show the variations of the first four structural natural frequencies for the composite flat wing models with $[30°]_4$ and $[45°]_4$ laminates, respectively. For the composite flat wings with $[30°]_4$ and $[45°]_4$ laminates, it can be observed from Figure 4 and Figure 5 that the first three frequencies are dominated by the bending displacements, and the fourth frequency displays torsional displacements. Afterwards, the experiment is conducted to validate the data presented in Table 3 using the test setup shown in previous Figure 3. The experimental results obtained from the accelerometer are plotted in Figure 6 and Figure 7 for the composite flat wing models with $[30°]_4$ and $[45°]_4$ laminates, respectively.

Table 3: Natural frequencies of composite flat wing at different fibre orientations

Fibre Orientation	Natural Frequency (rad/s)				Flutter Speed
	1	2	3	4	
$[30°]_4$	2.275	14.391	43.103	49.434	16.0 m/s
$[45°]_4$	2.0647	13.175	39.867	59.699	19.2 m/s

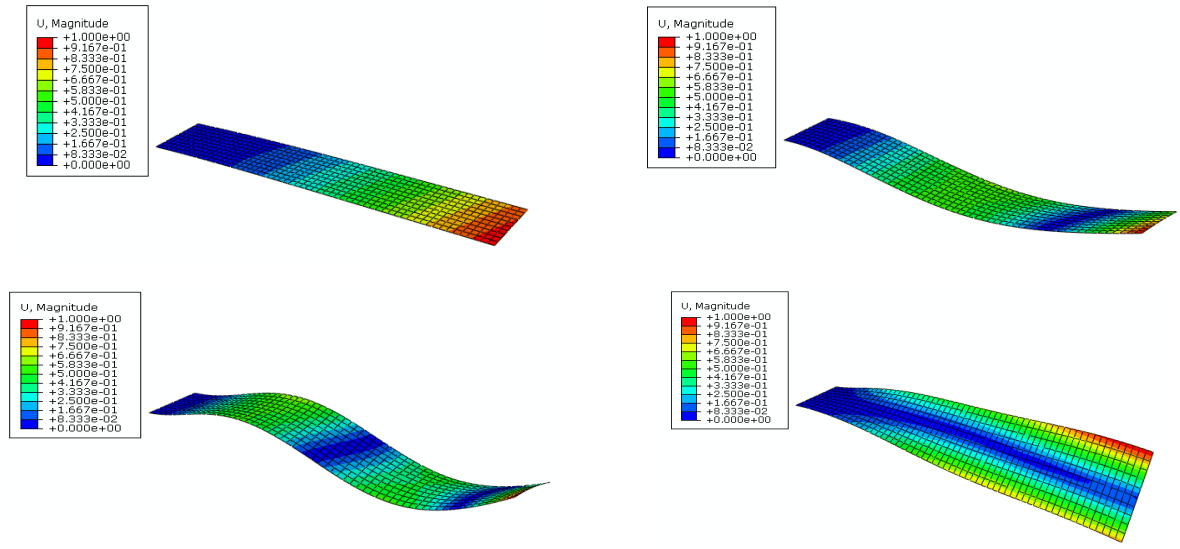

Figure 4: Natural frequencies and mode shapes of composite flat wing with $[30°]_4$

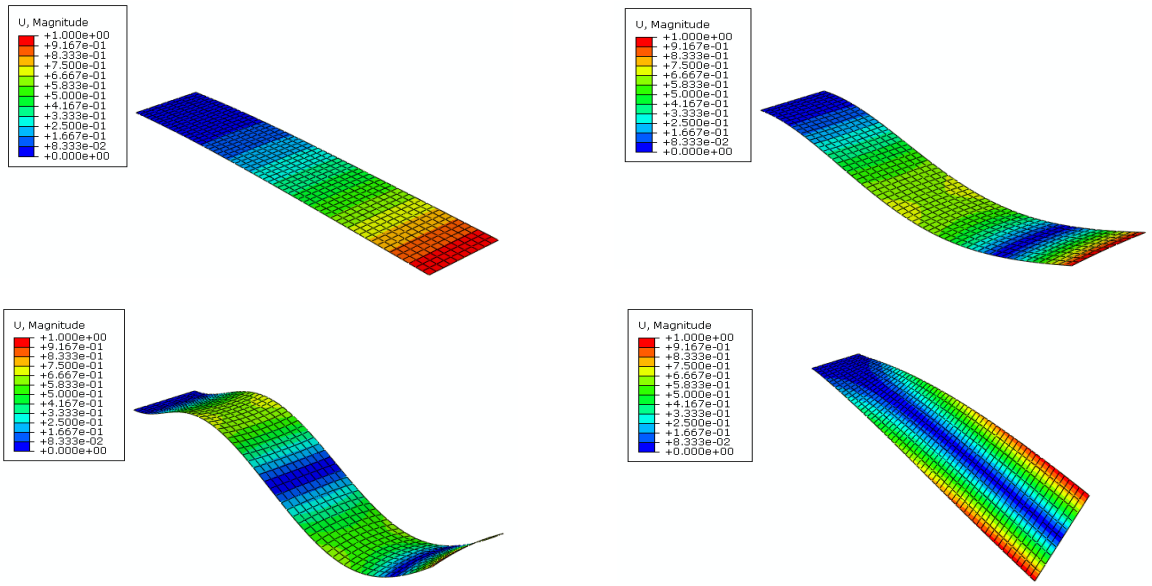

Figure 5: Natural frequencies and mode shapes of composite flat wing with $[45°]_4$

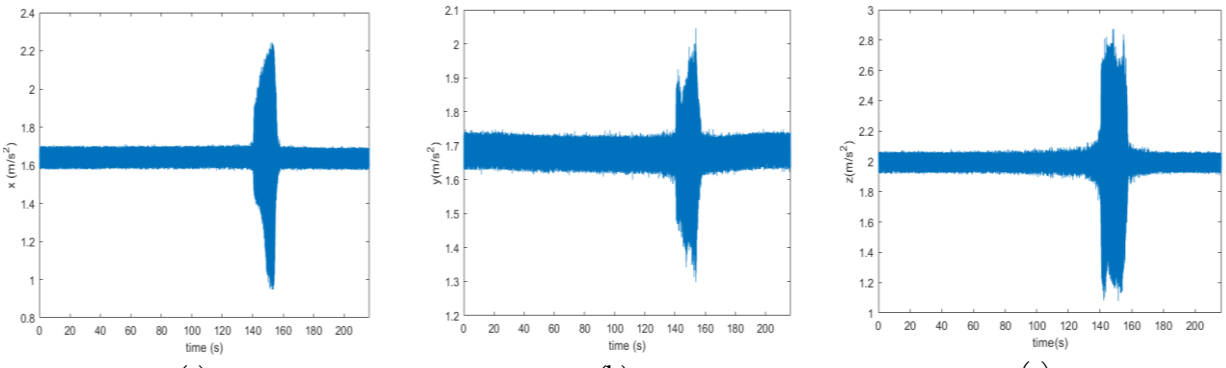

(a) (b) (c)

Figure 6: Accelerometer data for wing model with $[30°]_4$ laminate: (a) x-axis, (b) y-axis, (c) z-axis

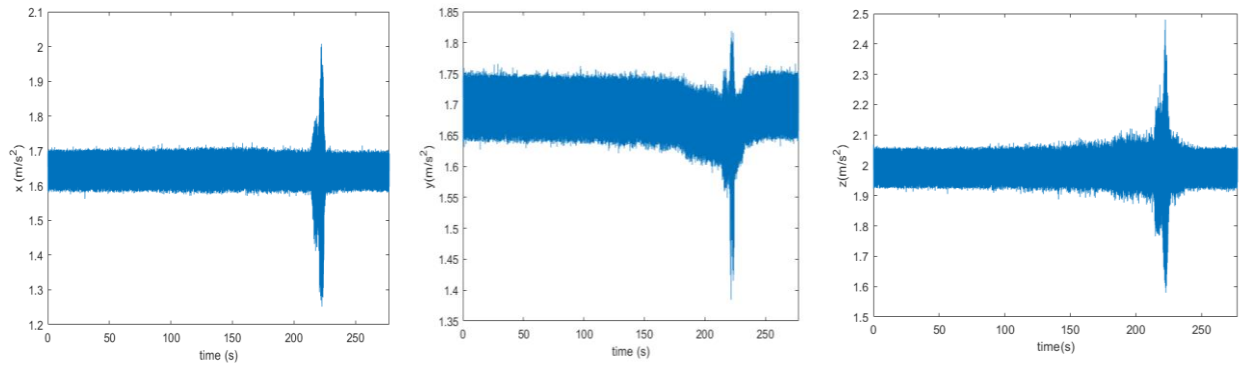

(a) (b) (c)

Figure 7: Accelerometer data for wing model with $[45°]_4$ laminate: (a) x-axis, (b) y-axis, (c) z-axis

The experimental results are recorded through an accelerometer sensor and video to observe the changes in displacement of the x-, y- and z- axes, as well as the vibration of the wing model when the wind tunnel's speed is increased from 0 m/s until the wing model starts to oscillate. Note that Figure 6 and Figure 7 present the recorded data along (a) x-axis, which is the chordwise direction of the wing, (b) y-axis, which is the spanwise direction, and (c) z-axis, which is the vertical direction. The peaks in the amplitude from Figures 6(a) and 6(b) indicate the occurrence of structural deformation in x- and y-axes while the amplitude peaks in Figure 6(c) implies vertical oscillations. It should be noted that the peak in Figure 6(c) coincides with the oscillations observed in the x- and y- axes, which shows that the wing model undergoes a complex three-dimensional motion as it reaches the flutter point within a time range between 140 to 160 seconds into the experiment, equivalent to 12.5 m/s wind speed. Similarly, from Figures 7(a), 7(b) and 7(c), the amplitude peaks of the x-, y- and z- axes can be observed between the time range of 210 to 240 seconds, equivalent to 19.0 m/s wind speed, which indicates the structural deformation has occurred at the flutter point.

The recorded data from the accelerometers and video footage is compared and correlated in order to obtain the flutter speed point. The result comparison between the experimental testing and the finite element analysis (FEA) are presented in Table 4. It shows clearly that the flutter speeds predicted by the FEA is higher than the experimental tests. For instances, the difference between the results of FEA and experiment tests for wing model with $[30°]_4$ laminate is 21.8% and $[45°]_4$ is 5.2%, respectively. This situation is likely due to the FEA software used in this study may not have fully captured the effects of bending-torsional coupling, which could be significantly for certain fiber orientations. Besides that, the result obtained has also shown that the flutter speed is significantly affected by the existence of bending-torsion coupling, which promotes the flutter to occur at a lower speed. This finding is also in line with the observation made by Mitra et al. [12]. Moreover, in comparison to pure laminate $[45°]_4$ that has the highest torsional rigidity [13], the flutter speed can be further increased up to 46%.

Table 4: Comparisons of flutter speed

Composite wing model	**Flutter Speed (m/s)**	
	FEA	**Experiment**
$[30°]_4$	16.0	12.5
$[45°]_4$	19.2	18.2

4. Conclusion

From the results and discussion of this studies, it is known that the cross-coupling parameters are important to be determined before conducting the analysis on composite laminates. The influence of this cross-coupling parameter can be seen during the analysis of structural natural frequencies and their mode shapes, especially for the fiber orientation between 5° and 40°. Higher cross-coupling parameters indicate a high coupling between bending and torsion. The inclusion of bending-torsion coupling has a significant effect on the structural vibration, which is shown to lead towards reduction of up to 31.3% of flutter speed as demonstrated from the difference in the results obtained from FEA and experimental analysis. It can be concluded that, to avoid the flutter phenomenon from occurring on composite wing at low speeds, it is necessary to design the composite wing with the inclusion of 45° plies as to enhance the torsional rigidity of the composite wing.

Acknowledgement

The authors highly acknowledge Universiti Teknologi Malaysia and Ministry of Education Malaysia for financial support to implement this research through UTMFR grant (Q.J130000.3851.21H92) and FRGS grant (R.J130000.7851.5F517).

References

[1] A. R. Collar, 'The Expanding Domain of Aeroelasticity', The Aeronautical Journal, vol. 50, no. 428, pp. 613-636, 1946.

[2] I. E. Garrick and W. H. Reed III, 'Historical Development of Aircraft Flutter', Journal of Aircraft, vol. 18, no. 11, pp. 897-912, 1981.

[3] J. R. Wright and J. E. Cooper, Introduction to Aircraft Aeroelasticity and Loads, John Wiley & Sons, 2008.

[4] M. S. Othman, O. T. Chun, M. Y. Harmin and F. I. Romli, 'Aeroelastic Effects of a Simple Rectangular Wing-Box Model with Varying Rib Orientations', IOP Conference Series: Materials Science and Engineering, vol. 152, no. 1, 012009, 2016.

[5] T. Farsadi and J. J. Hasbestan, 'Calculation of Flutter and Dynamic Behavior of Advanced Composite Swept Wings with Tapered Cross Section in Unsteady Incompressible Flow', Mechanics of Advanced Materials and Structures, vol. 26, no. 4, pp. 314-332, 2019.

[6] T. K. Jun, M. Y. Harmin and F. I. Romli, 'Aeroelastic Tailoring of Composite Wing Design Using Bee Colony Optimisation', Applied Mechanics and Materials, vol. 629, pp. 182-188, 2014.

[7] S. G. P. Castro, T. A. M. Guimarães, D. A. Rade and M. V. Donadon, 'Flutter of Stiffened Composite Panels Considering the Stiffener's Base as a Structural Element', Composite Structures, vol. 140, pp. 36-43, 2016.

[8] G. A. Georghiades and J. R. Banerjee, 'Flutter Prediction for Composite Wings using Parametric Studies', AIAA Journal, vol. 35, no. 4, pp. 746-748, 1997.

[9] S. J. Hollowell and J. Dugundji, 'Aeroelastic Flutter and Divergence of Stiffness Coupled, Graphite/Epoxy Cantilevered Plates', Journal of Aircraft, vol. 21, no. 1, pp. 69-76, 1984.

[10] T. A. Weisshaar and R. J. Ryan, 'Control of Aeroelastic Instabilities Through Stiffness Cross-Coupling', Journal of Aircraft, vol. 23, no. 2, pp. 148-155, 1986.

[11] A. Attaran, D. L. Majid, S. Basri, A. S. Mohd Rafie and E. J. Abdullah, 'Structural Optimization of an Aeroelastically Tailored Composite Flat Plate Made of Woven Fiberglass/Epoxy', Aerospace Science and Technology, vol. 15, no. 5, pp. 393-401, 2011.

[12] A. Mitra and A. Chakraborty, 'Multi-objective Optimization of Composite Airfoil Fibre Orientation Under Bending–Torsion Coupling for Improved Aerodynamic Efficiency of

Horizontal Axis Wind Turbine Blade', Journal of Wind Engineering and Industrial Aerodynamics, vol. 221, 104881, 2022.

[13] A. Viglietti, E. Zappino and E. Carrera, 'Free Vibration Analysis of Variable Angle-Tow Composite Wing Structures', Aerospace Science and Technology, vol. 92, pp. 114-125, 2019.